Single-molecule measurements of the effect of force on Thy-1/αvβ3-integrin interaction using nonpurified proteins

Francesca Burgos-Bravo[a,b], Nataniel L. Figueroa[c], Nathalie Casanova-Morales[d], Andrew F. G. Quest[a,b], Christian A. M. Wilson[d,*], and Lisette Leyton[a,b,*]

[a]Cellular Communication Laboratory, Programa de Biología Celular y Molecular, Instituto de Ciencias Biomédicas, Facultad de Medicina, Universidad de Chile, 838-0453 Santiago, Chile; [b]Advanced Center for Chronic Diseases (ACCDiS), Center for Studies of Exercise, Metabolism and Cancer, Instituto de Ciencias Biomédicas, Facultad de Medicina, Universidad de Chile, 838-0453 Santiago, Chile; [c]Physics Department, Pontificia Universidad Católica de Chile, 782-0436 Santiago, Chile; [d]Biochemistry and Molecular Biology Department, Facultad de Ciencias Químicas y Farmacéuticas, Universidad de Chile, 838-0494 Santiago, Chile

ABSTRACT **Thy-1 and αvβ3 integrin mediate bidirectional cell-to-cell communication between neurons and astrocytes. Thy-1/αvβ3 interactions stimulate astrocyte migration and the retraction of neuronal prolongations, both processes in which internal forces are generated affecting the bimolecular interactions that maintain cell–cell adhesion. Nonetheless, how the Thy-1/αvβ3 interactions respond to mechanical cues is an unresolved issue. In this study, optical tweezers were used as a single-molecule force transducer, and the Dudko-Hummer-Szabo model was applied to calculate the kinetic parameters of Thy-1/αvβ3 dissociation. A novel experimental strategy was implemented to analyze the interaction of Thy-1-Fc with nonpurified αvβ3-Fc integrin, whereby nonspecific rupture events were corrected by using a new mathematical approach. This methodology permitted accurately estimating specific rupture forces for Thy-1-Fc/αvβ3-Fc dissociation and calculating the kinetic and transition state parameters. Force exponentially accelerated Thy-1/αvβ3 dissociation, indicating slip bond behavior. Importantly, nonspecific interactions were detected even for purified proteins, highlighting the importance of correcting for such interactions. In conclusion, we describe a new strategy to characterize the response of bimolecular interactions to forces even in the presence of nonspecific binding events. By defining how force regulates Thy-1/αvβ3 integrin binding, we provide an initial step towards understanding how the neuron–astrocyte pair senses and responds to mechanical cues.**

Monitoring Editor
Margaret Gardel
University of Chicago

Received: Mar 3, 2017
Revised: Oct 10, 2017
Accepted: Dec 1, 2017

INTRODUCTION

Cell adhesion, the ability of a cell to bind either to another cell or to the extracellular matrix (Gumbiner, 1996), plays an important role in cell communication and the regulation of many biological processes, including cell proliferation, migration, and survival (Khalili and Ahmad, 2015). In the CNS, cellular adhesion between neurons and astrocytes is critical to regulating neuronal functions, both under physiological conditions as well as in response to CNS damage (Benarroch, 2005). Astrocytes are the most abundant type of glial cells in the CNS and exceed more than fivefold the quantity of neurons (Sofroniew and Vinters, 2010). A single astrocyte can contact up to 10^5 synapses (Bushong *et al.*, 2002) and hundreds of dendrites (Halassa, Fellin, *et al.*, 2007); hence, a wide variety of molecular interactions mediate the communication between neurons and glial cells.

Our group has previously reported that the glycosyl phosphatidylinositol (GPI)-anchored Thy-1, an abundant neuronal cell adhesion protein from the immunoglobulin (Ig) superfamily

This article was published online ahead of print in MBoC in Press (http://www.molbiolcell.org/cgi/doi/10.1091/mbc.E17-03-0133) on December 6, 2017.

*Address correspondence to: Lisette Leyton (lleyton@med.uchile.cl) and Christian A. M. Wilson (yitowilson@gmail.com).

Abbreviations used: DHS, Dudko-Hummer-Szabo; k_{off}^0, off-rate constant at zero force; $\Delta G^{\ddagger}$, free energy of activation; $\Delta x^{\ddagger}$, distance to the transition state; τ^0, bond lifetime at zero force.

© 2018 Burgos-Bravo *et al.* This article is distributed by The American Society for Cell Biology under license from the author(s). Two months after publication it is available to the public under an Attribution–Noncommercial–Share Alike 3.0 Unported Creative Commons License (http://creativecommons.org/licenses/by-nc-sa/3.0).

"ASCB®," "The American Society for Cell Biology®," and "Molecular Biology of the Cell®" are registered trademarks of The American Society for Cell Biology.

(Leyton and Hagood, 2014), acts as a receptor for the astrocytic αvβ3 integrin (Leyton *et al.*, 2001; Hermosilla *et al.*, 2008). This heterodimeric integrin is upregulated in astrocytes after CNS injury due to increased inflammation (Ellison *et al.*, 1999). We have also provided evidence for a direct Thy-1/αvβ3 integrin interaction mediated by the integrin-binding site (RLD) in Thy-1 using surface plasmon resonance analysis with the functional Fc-tagged fusion proteins Thy-1-Fc and αvβ3-Fc (Hermosilla *et al.*, 2008). Furthermore, we have described that the Thy-1/αvβ3 integrin interaction mediates bidirectional neuron-to-astrocyte communication, inducing cell migration in astrocytes (Avalos, Valdivia, *et al.*, 2009; Kong, Munoz, *et al.*, 2013) and promoting an inhibition of neurite outgrowth and retraction of already established neuronal processes in neurons (Herrera-Molina *et al.*, 2012; Maldonado *et al.*, 2016). Therefore, this interaction might play a key role in the responses of both neurons and astrocytes after CNS injury.

Adhesion proteins that maintain cell–cell communication, such as Ig superfamily members and integrins, are constantly exposed to mechanical forces generated as a consequence of different cellular functions (Evans and Calderwood, 2007; Strunz *et al.*, 2000; Liu *et al.*, 2015). In the wound healing process, for instance, cells tug on each other during migration and exert traction forces on the interactions that maintain cell–cell adhesion (Ananthakrishnan and Ehrlicher, 2007; Rakshit and Sivasankar, 2014). As mentioned, astrocyte migration is a process triggered by the Thy-1/αvβ3 integrin interaction. In cell migration, the polymerization of actin filaments and the sliding of the motor protein myosin II over these filaments generate contractile forces. In turn, these forces pull on the cell body to promote forward motion and retraction of the cell rear (Pollard and Borisy, 2003; Fournier *et al.*, 2010). Similarly, neurite retraction also occurs due to increased contraction of the cortical actin cytoskeleton (Kranenburg *et al.*, 1997; Govek *et al.*, 2005; Maldonado *et al.*, 2016). Therefore, both cell migration and neurite retraction generate internal forces exerted to protein–protein interactions that maintain cell–cell adhesion, as is the case of neuronal Thy-1 and astrocytic αvβ3 integrin binding.

Force can tilt the energy landscape of the dissociation pathway, alter the height of the energy barrier, and modify unbinding kinetics, that is, forces that regulate molecular interactions by modulating the off-rate (k_{off}) (Bell, 1978; Dembo *et al.*, 1988). Based on how bimolecular interactions respond to mechanical forces, bonds can be classified as either slip bonds, where force shortens bond lifetime (accelerate dissociation); catch bonds, where force prolongs bond lifetime (slow down dissociation); or ideal bonds, where bond lifetime is independent of force (Dembo *et al.*, 1988; Zhu, 2014). Mechanical cues from the surrounding environment clearly influence binding properties and, consequently, modify the effects of cellular signaling, as triggered by adhesion proteins such as Thy-1 and αvβ3 integrin. Bidirectional neuron-to-astrocyte communication in the CNS could therefore also be affected. Nonetheless, how mechanical forces may modulate kinetic parameters of the interaction between Thy-1 and αvβ3 integrin has never been explored. Therefore, molecular force spectroscopy was used in the present study to characterize the mechanical properties of the Thy-1/αvβ3 integrin interaction at the single-molecule level. This methodology has been employed to characterize protein–protein interactions in response to forces, resulting in assessments of bond strength, the dissociation process energy landscape, and the lifetime of bimolecular interactions (Yuan *et al.*, 2000; Stangner *et al.*, 2013).

In the current study, optical tweezers and force-ramp assays were used to obtain rupture force data for the Thy-1/αvβ3 integrin interaction. The kinetic parameters of the force-induced Thy-1/αvβ3 dissociation were determined using the Dudko-Hummer-Szabo (DHS) model (Dudko *et al.*, 2008). Previous studies using molecular force spectroscopy to characterize the effect of mechanical forces on bimolecular interactions have utilized purified proteins to reduce the possibility of nonspecific interactions (Zhang *et al.*, 2004; Litvinov *et al.*, 2005; Stangner *et al.*, 2013). However, protein purification may represent a limiting factor. To overcome this limitation, we designed experimental and mathematical strategies for performing assessments with the nonpurified αvβ3-Fc fusion protein (i.e., directly from crude supernatant of transfected cells). Through this, more accurate kinetic and thermodynamic unbinding parameters at the single-molecule level of the Thy-1/αvβ3 dissociation were obtained even when nonspecific rupture events were detected. Additionally, a slip bond behavior for the bimolecular interaction between Thy-1 and αvβ3 integrin was identified. The parameters obtained were confirmed using purified αvβ3 integrin. Of note, nonspecific interactions were detected even for purified proteins, meaning that our mathematical approach might also be of use when working with purified proteins.

RESULTS

Rupture force measurements and the specificity of the Thy-1 and αvβ3 integrin interaction

The optical tweezers technique (miniTweezers) (Smith *et al.*, 2003) was used to determine the binding parameters between Thy-1 and αvβ3 integrin at the single-molecule level in response to pulling forces. Fc-tagged recombinant molecules were bound to protein G-coated polystyrene beads for the force spectroscopy experiments (see Figure 1A for schematic representation). To promote the Thy-1-Fc/αvβ3-Fc interaction, the optically trapped bead coated with αvβ3-Fc was approached to the micropipette-attached bead coated with Thy-1-Fc. If a protein-protein interaction occurs, then the optically trapped bead is displaced from the center, and force is generated. When the generated force is greater than the force that disrupts the bond, rupturing of the interaction ensues. The rupture force is obtained from a force-trap position trace (Figure 1A).

To characterize the binding parameters of the interaction between purified Thy-1-Fc and αvβ3-Fc integrin in supernatants using molecular force spectroscopy, single-molecule interactions are needed. Therefore, it was first necessary to estimate the concentration of αvβ3-Fc in the supernatants, with specific focus on determining the lowest concentration required for single-molecule binding events with Thy-1. Considering that supernatants obtained from HEK293T cells transfected with αvβ3-Fc contained other proteins (Supplemental Figure S1A), a semiquantitative Western blot analysis was performed using antibodies against the Fc fragment (Supplemental Figure S1B). Applying the linear regression equation (Supplemental Figure S1C) and a molecular weight of ~300 kDa for the αvβ3-Fc molecule, the concentration obtained for the αvβ3-Fc integrin in the supernatant was 4 nM. Subsequently, different dilutions of the supernatant containing the αvβ3-Fc fusion protein (without dilution, 10^3-, 10^6-, and 10^9-fold dilutions) were incubated with protein G-beads to define the lowest concentration needed for single-molecule binding events between Thy-1-Fc and αvβ3-Fc. Since many different proteins were present in the HEK293T cell–based supernatant, we recognized some might compete with αvβ3-Fc to interact with Thy-1. Such interactions would generate nonspecific binding events, which might partially obscure the signals of the specific interaction between Thy-1-Fc and αvβ3-Fc. To try and limit measurements to only specific-binding events, protein G was used to specifically bind αvβ3-Fc to the beads. To test whether nonspecific binding events persisted despite this measure, and to estimate

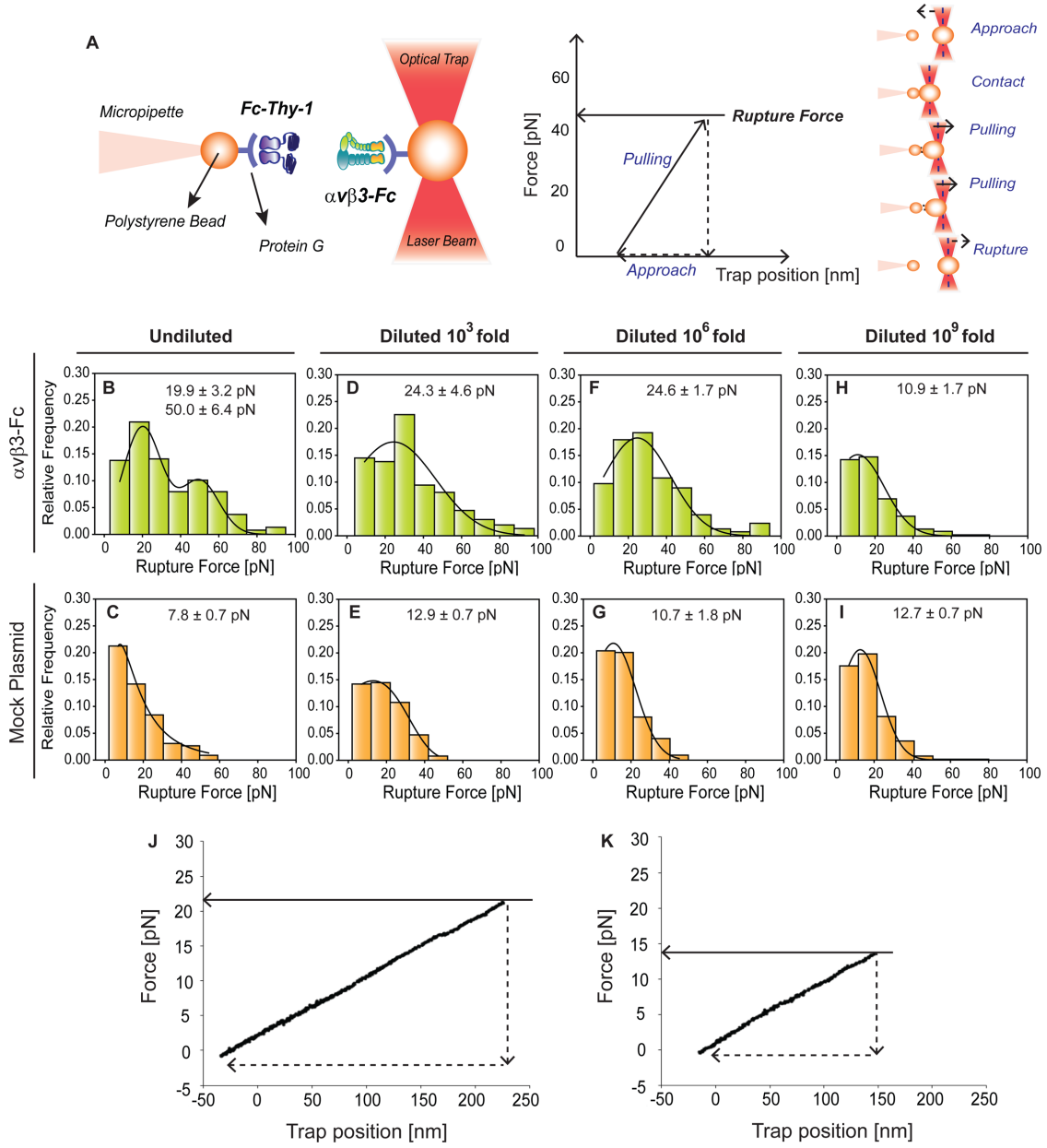

FIGURE 1: Rupture force measurements for specific and nonspecific Thy-1-Fc interactions with different supernatant dilutions with or without αvβ3-Fc integrin using an optical tweezers system. (A) Scheme of the optical tweezers technique used to study the Thy-1-Fc/αvβ3-Fc interaction. Left, MiniTweezers experimental design. Two different sizes of protein G-coated beads were used; the smaller bead (2.1 μm) contained purified Thy-1-Fc and was attached to a micropipette by suction, whereas the larger bead (3.1 μm) contained the αvβ3-Fc protein and was trapped by a laser beam and held in the focus of the microscope. Right, force-trap position trace for one approach-retraction cycle. To promote protein interaction, the laser beam-trapped bead contacted the other bead (approach). After <1 s of contact, the beads were separated by pulling the laser beam-trapped bead at a constant force-loading rate (10 pN/s) (retraction) until interaction rupturing. Dashed lines in the red laser beam represent the center of the optical trap. (B–I) Rupture force histograms obtained for interactions between (B, D, F, and H) Thy-1-Fc/αvβ3-Fc integrin supernatant or (C, E, G, and I) Thy-1-Fc/mock plasmid supernatant, at different dilutions. (B, C) Undiluted supernatants or supernatants diluted (D, E) 10^3-fold, (F, G) 10^6-fold, or (H, I) 10^9-fold. All histograms summarize at least 300 binding events per five pairs of new beads. Solid line corresponds to a Gaussian distribution curve used to illustrate the distribution of rupture forces and characterize the peak rupture force. Representative force-trap position traces obtained from MiniTweezers measurements between Thy-1-Fc and the supernatant (J) containing the αvβ3-Fc integrin or (K) from cells transfected with mock plasmid, both diluted 10^6-fold.

the magnitude of such events, the supernatant of HEK293T cells transfected with an empty plasmid vector was used as a control (mock plasmid). The absence of αvβ3-Fc integrin in this control supernatant was confirmed by Western blotting (Supplemental Figure S1, A and B). The mock supernatant was diluted just as the αvβ3-Fc-containing supernatants.

When using the undiluted supernatant containing αvβ3-Fc, the resulting rupture forces showed bimodal distribution, the peaks of which (19.9 ± 3.2 and 50.0 ± 6.4 pN) were indicative of multiple binding events (Figure 1B). However, only the lower peak rupture force, characteristic of single-molecule interactions, was detected following dilution of the αvβ3-Fc-containing supernatant (Figure 1, D, F, and H). On the other hand, similar rupture force distributions were found in all spectroscopy experiments using different mock-supernatant dilutions (Figure 1, C, E, G, and I), suggesting that Thy-1-Fc promotes nonspecific interactions characterized by low rupture forces (~10 pN). Differences between the rupture force histograms obtained for Thy-1-Fc/αvβ3-Fc and Thy-1-Fc/mock plasmid were only detected up to a 10^6-fold dilution (Figure 1, F and G). The representative force-trap position traces obtained for the 10^6 dilutions of both Thy-1-Fc/ αvβ3-Fc and Thy-1-Fc/mock plasmid are shown in Figure 1, J and K, respectively. Indeed, when the αvβ3-Fc was diluted 10^9-fold, the histogram profile and peak rupture force were similar to that obtained for the Thy-1-Fc/mock plasmid (Figure 1, H and I). These results indicate that a 10^6-fold dilution of the αvβ3-Fc-containing supernatant would be the most diluted condition at which rupture forces differ from the control (i.e., Thy-1-Fc/mock plasmid). Consequently, this concentration would also represent the highest dilution at which specific Thy-1-Fc/αvβ3-Fc interactions could be detected. Therefore, the 10^6-fold dilution was defined as the most diluted condition needed for specific single-molecule binding events between Thy-1-Fc and αvβ3-Fc integrin. These results also suggest the presence of nonspecific binding events, despite that the designed experimental strategy to evaluate purified Thy-1-Fc and αvβ3-Fc interactions in supernatants used protein-G to specifically bind the αvβ3-Fc integrin to the beads.

Adhesion frequency measurements and the specificity of the Thy-1 and αvβ3 integrin interaction

Adhesion frequency was determined to improve the characterization of binding specificity between Thy-1-Fc and the αvβ3-Fc integrin obtained from the supernatant of transfected cells. Adhesion frequency, the probability for adhesion based on the total number of contacts, constitutes a measure of the relative on-rate value (Robert *et al.*, 2007). Evaluating this parameter helps discriminate between specific and nonspecific interaction events. The adhesion frequency was evaluated using either undiluted or diluted supernatants (10^3-, 10^6-, and 10^9-fold) for either the αvβ3-Fc-containing (Thy-1-Fc/αvβ3-Fc) or control supernatant (Thy-1-Fc/mock plasmid) (Figure 2A). The highest adhesion frequency was observed for the interaction between Thy-1-Fc and the undiluted supernatant containing αvβ3-Fc (Figure 2A). Values for adhesion frequencies of supernatants at the 10^3- and 10^6-fold dilutions tended to decrease with respect to those obtained for the nondiluted supernatant; however, the differences were not statistically significant. A significant decrease in the adhesion frequency was observed for the interaction between Thy-1-Fc and the αvβ3-Fc integrin at the 10^9 dilution. Considering the similarity of this value with those of the adhesion frequency determined for Thy-1-Fc and the mock supernatants (Figure 2A), these results indicate that the binding events occurring between Thy-1-Fc and the αvβ3-Fc integrin-containing supernatant at the 10^9 dilution are due exclusively to nonspecific interactions (compare green bar at 10^9 dilution with orange bars, Figure 2A).

To corroborate the specific binding events between Thy-1-Fc/αvβ3-Fc integrin at the single-molecule level (i.e., αvβ3-Fc at a 10^6-fold dilution), the interaction was characterized using a supernatant predepleted of the αvβ3-Fc integrin (see *Materials and Methods* and Supplemental Figure S2A). Predepletion of the αvβ3-Fc integrin

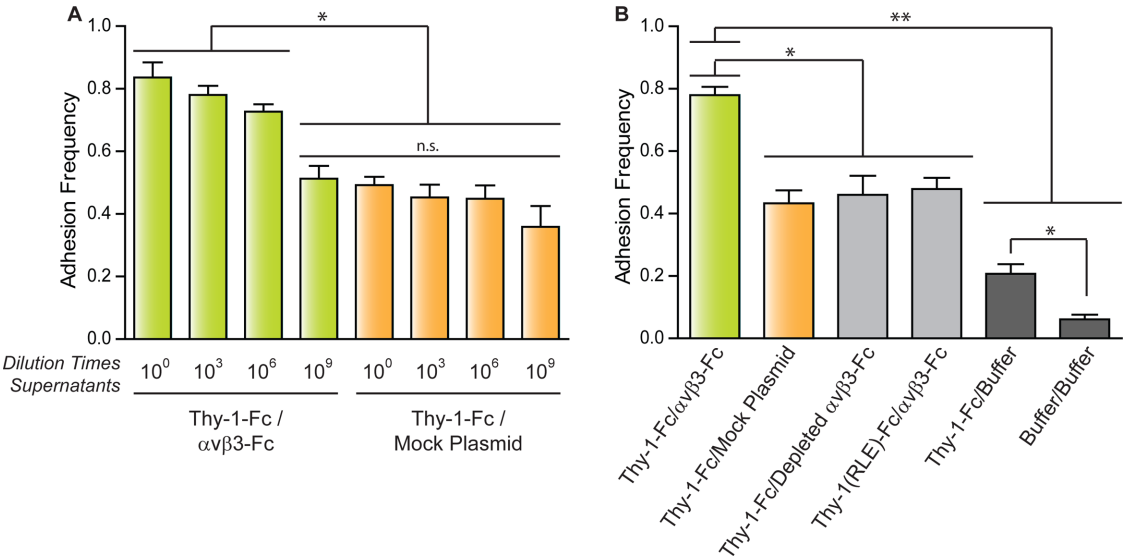

FIGURE 2: Adhesion frequency of pure Thy-1-Fc with supernatants with or without αvβ3-Fc integrin. Adhesion frequency was assessed by measuring the number of total binding events in at least 50 approach-retraction cycles per five pairs of freshly prepared beads. (A) Adhesion frequency of Thy-1-Fc measured in different dilutions of the supernatant containing the αvβ3-Fc protein (αvβ3-Fc) or the supernatant from cells transfected with mock plasmids (Mock Plasmid). (B) As a control for nonspecific interactions, adhesion frequency was also evaluated between Thy-1-Fc and the supernatant depleted of the αvβ3-Fc integrin (Depleted αvβ3-Fc) or with the HEPES buffer (Buffer), as well as between Thy-1(RLE)-Fc mutated in the integrin binding-site and the supernatant containing the αvβ3-Fc (αvβ3-Fc). The binding frequency between the two types of beads was also tested (Buffer/Buffer). Data are expressed as the mean ± SEM (*$p < 0.05$; **$p < 0.01$; n.s., nonsignificant).

decreased the adhesion frequency of Thy-1-Fc/depleted αvβ3-Fc by ~30% compared with the Thy-1-Fc/αvβ3-Fc condition (Figure 2B). As expected, the adhesion frequency between Thy-1-Fc and the αvβ3-Fc-depleted supernatant was equivalent to that obtained for the Thy-1-Fc/mock plasmid (Figure 2B). These results suggest that depletion of the fusion protein from the supernatant eliminates the specific binding events between Thy-1-Fc and the αvβ3-Fc integrin and that nonspecific interactions occurring in Thy-1-Fc/depleted αvβ3-Fc are comparable to those in Thy-1-Fc/mock supernatant.

As a second strategy to corroborate specific binding between Thy-1-Fc and αvβ3-Fc, we used the Thy-1(RLE)-Fc protein, which is mutated in the integrin binding site (RLD) (Hermosilla *et al.*, 2008). The interaction of this protein was tested with the αvβ3-Fc supernatant. As anticipated, a lower adhesion frequency than that calculated for wild-type Thy-1-Fc was detected, similar to what was observed when nonspecific binding was evaluated (Figure 2B). These results confirm the specific interaction of Thy-1 with αvβ3-Fc and indicate that nonspecific binding events are independent of the Thy-1integrin-binding site.

Additionally, to study whether nonspecific interactions depended on Thy-1-Fc and the protein G-beads, the adhesion frequency was evaluated between Thy-1-Fc and protein G-beads preincubated only with the HEPES buffer (Thy-1-Fc/buffer). A different control included measuring the interaction using beads incubated only with buffer (buffer/buffer). The adhesion frequency between Thy-1-Fc and the uncoated protein G-beads was ~53% lower than the condition with supernatant from cells transfected with mock plasmid (i.e., Thy-1-Fc/buffer vs. Thy-1-Fc/mock plasmid, Figure 2B). Notably, a significant decrease in adhesion frequency also occurred with uncoated protein G-beads (i.e., Thy-1-Fc/buffer vs. buffer/buffer, Figure 2B), suggesting that Thy-1-Fc interacts not only with soluble proteins present in the supernatant from transfected cells, but also with the protein G-beads alone. Importantly, these results suggest that of the total binding events found in the single-molecule approach, performed with Thy-1-Fc and nonpurified αvβ3-Fc integrin, only ~30% are attributable to specific interactions between Thy-1-Fc and the integrin.

Correction for rupture forces from nonspecific binding events and estimation of Thy-1-Fc/αvβ3-Fc binding parameters

The binding parameters of the Thy-1/αvβ3-Fc integrin interaction can be obtained from the rupture force distribution graph (Figure 1F) by applying the DHS model (Dudko *et al.*, 2008). The experimental setup provided rupture forces representative of both specific and nonspecific binding. Therefore, to characterize the correct binding parameters between Thy-1-Fc and the αvβ3-Fc integrin, the rupture forces generated by nonspecific binding were filtered from the total rupture forces obtained in the supernatant for the interaction between pure Thy-1-Fc and the αvβ3-Fc.

To estimate the effects of nonspecific binding events, the rupture forces were measured for supernatant interactions of Thy-1-Fc/mock-transfected cells. The presence of only nonspecific binding events in this condition was corroborated by characterizing rupture forces between Thy-1-Fc and supernatants depleted of αvβ3-Fc (Supplemental Figure S3A). Rupture forces were also characterized between the mutant Thy-1(RLE)-Fc and supernatant containing αvβ3-Fc (Supplemental Figure S3B). As expected, both conditions showed rupture force distributions and peak rupture forces equivalent to those obtained for Thy-1-Fc and the supernatant from cells transfected with mock plasmid (Figure 1G). These results are consistent with those depicted in Figure 2B, where similar adhesion frequency values were obtained for each condition in which nonspecific interactions were observed.

To correct nonspecific rupture forces from the total rupture forces obtained for Thy-1-Fc/αvβ3-Fc in the supernatant interaction, a mathematical strategy was developed (see *Materials and Methods* and the Supplemental Material). Briefly, the assumption was that the total rupture forces measured between Thy-1 and the mock supernatant must have resulted from only nonspecific binding events, which occur with the probability $P(\overline{AB})$ (Figure 3A). On the other hand, the total rupture forces measured in the supernatant containing αvβ3-Fc must have resulted from both nonspecific and specific binding events. The probability of nonspecific events remained $P(\overline{AB})$, while that of specific binding events was defined by $P(AB)$ (Figure 3B). Since both events are exclusive and complementary, $P(\overline{AB}) + P(AB) = 1$, thus allowing calculation for the value of $P(AB)$.

To determine the contribution of specific Thy-1-Fc/αvβ3-Fc interactions to the rupture forces measured in the Thy-1-Fc/αvβ3-Fc-containing supernatant, the measured rupture forces were weighted by the probability $P(AB)$. After applying this mathematical correction, a rupture force histogram representative of only specific interactions between Thy-1-Fc and the αvβ3-Fc integrin was obtained (Figure 3C). Fitting with a Gaussian distribution curve resulted in a peak rupture force of 25.4 ± 1.6 pN.

Thy-1-Fc/αvβ3-Fc interaction lifetimes were calculated for each bin of the rupture force histogram by applying the DHS model (Eq. 1; see *Materials and Methods*; Figure 3D). The lifetime data were then fitted by applying the nonlinear DHS model (Eq. 2; see *Materials and Methods*), thus characterizing the energy landscape of the unbinding process between Thy-1-Fc and the αvβ3-Fc integrin (Figure 3E). Bond lifetime values ($\tau^0 = 19.30 \pm 1.34$ s), the off-rate constant ($k_{off}^0 = 0.051 \pm 0.003$ s^{-1}), the distance to the transition state ($\Delta x^{\ddagger} = 0.50 \pm 0.05$ nm), and the free energy of activation ($\Delta G^{\ddagger} = 5.54 \pm 0.47\ k_BT$) were calculated in the absence of force. Therefore, the applied experimental and mathematical strategies allowed us to characterize the force-dependent kinetic parameters of the dissociation process between Thy-1 and αvβ3 integrin, despite using a nonpurified integrin.

Experimental validation of the mathematical strategy used to obtain binding parameters for interactions between purified and nonpurified proteins

To validate the implemented mathematical approach, the αvβ3-Fc integrin was purified to study the interaction parameters between Thy-1-Fc and the pure αvβ3-Fc fusion protein under force. Previous attempts to purify the αvβ3-Fc fusion protein have generated a nonfunctional and unstable integrin (Hermosilla *et al.*, 2008). Therefore, mutations were introduced into the C_H3 domains of the Fc fragment, as described to purify α5β1-Fc (Coe *et al.*, 2001). These mutations reportedly improve the possibility of maintaining functional heterodimers after purification. SDS–PAGE with silver staining revealed the presence of αv-Fc and β3-Fc subunits, as well as other proteins with greater electrophoretic mobility in the supernatant obtained from transfected cells. However, only αv-Fc and β3-Fc subunits were detected after purification (Supplemental Figure S4A). Additionally, the purified product was also detected by Western blotting using antibodies against the Fc fragment. Western blotting analyses of the eluates were performed using antibodies against the Fc fragment under reducing and nonreducing conditions. The αv-Fc and β3-Fc subunits were found under reducing conditions, while the αvβ3-Fc heterodimer was found in nonreducing conditions (Supplemental Figure S4, B and C).

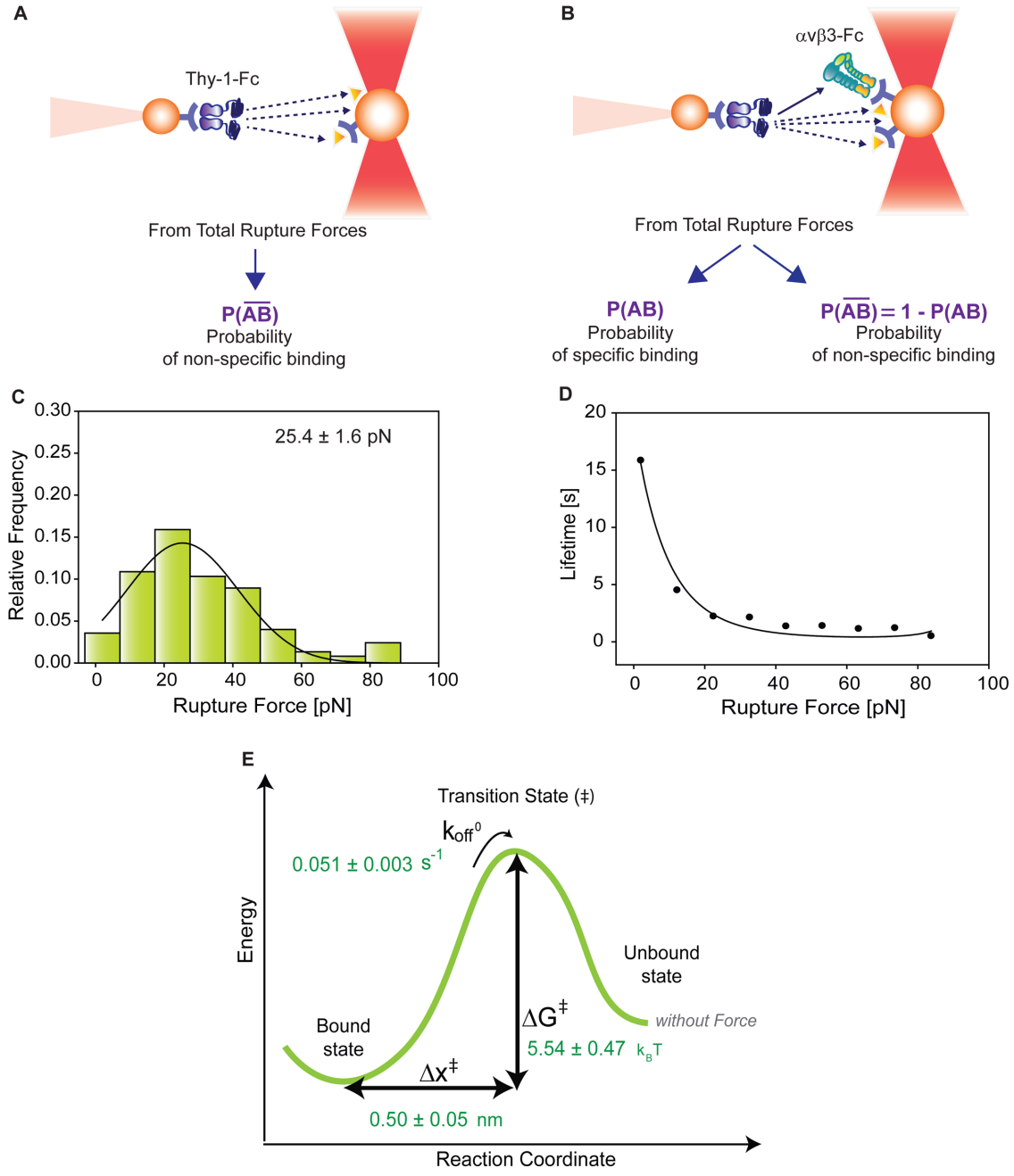

FIGURE 3: Correction for nonspecific rupture events and quantification of the binding parameters between pure Thy-1-Fc and αvβ3-Fc integrin in supernatant. To obtain rupture forces representative of only specific binding events between Thy-1-Fc and the αvβ3-Fc integrin, we developed a mathematical strategy (see *Materials and Methods*) to correct rupture forces resulting from nonspecific binding events. Assumptions made: (A) from the total rupture forces observed between Thy-1-Fc and beads preincubated with supernatant from cells transfected with mock plasmid, where $P(\overline{AB})$ indicated the probability of a nonspecific binding (dashed line arrows) and (B) from the total rupture forces observed between Thy-1-Fc and supernatant containing αvβ3-Fc, where $P(\overline{AB})$ indicated the probability of a nonspecific binding and $P(AB)$ indicated the probability for specific binding interactions (solid line arrow). (C) Resulting rupture force histogram after applying mathematical corrections, representative of only specific Thy-1-Fc/αvβ3-Fc interactions. Black line in the histogram corresponds to a Gaussian distribution curve used to illustrate the distribution and peak of rupture forces. (D) Force-dependent lifetime for Thy-1-Fc/αvβ3-Fc binding estimated from each bin shown in C, using the the Dudko-Hummer-Szabo model (Eq. 1; see *Materials and Methods*). Solid line in D corresponds to the fitted curve obtained using Eq. 2 (see *Materials and Methods*; $\upsilon = 0.5$). (E) Energy landscape of the unbinding process between Thy-1-Fc and the αvβ3-Fc integrin in the supernatant, where off-rate at zero force (k_{off}^0), distance to the transition state ($\Delta x^{\ddagger}$), and the free energy of activation ($\Delta G^{\ddagger}$) are shown.

To test whether functionality of the αvβ3-Fc protein was maintained after purification, an enzyme-linked immunosorbent assay was used. In this assay, the nonpurified and pure αvβ3-Fc fusion proteins bound to known RGD-containing ligands, including fibronectin, vitronectin, and the Kis peptide (Leyton *et al.*, 2001). Nevertheless, binding did not occur with RGE-containing peptides,

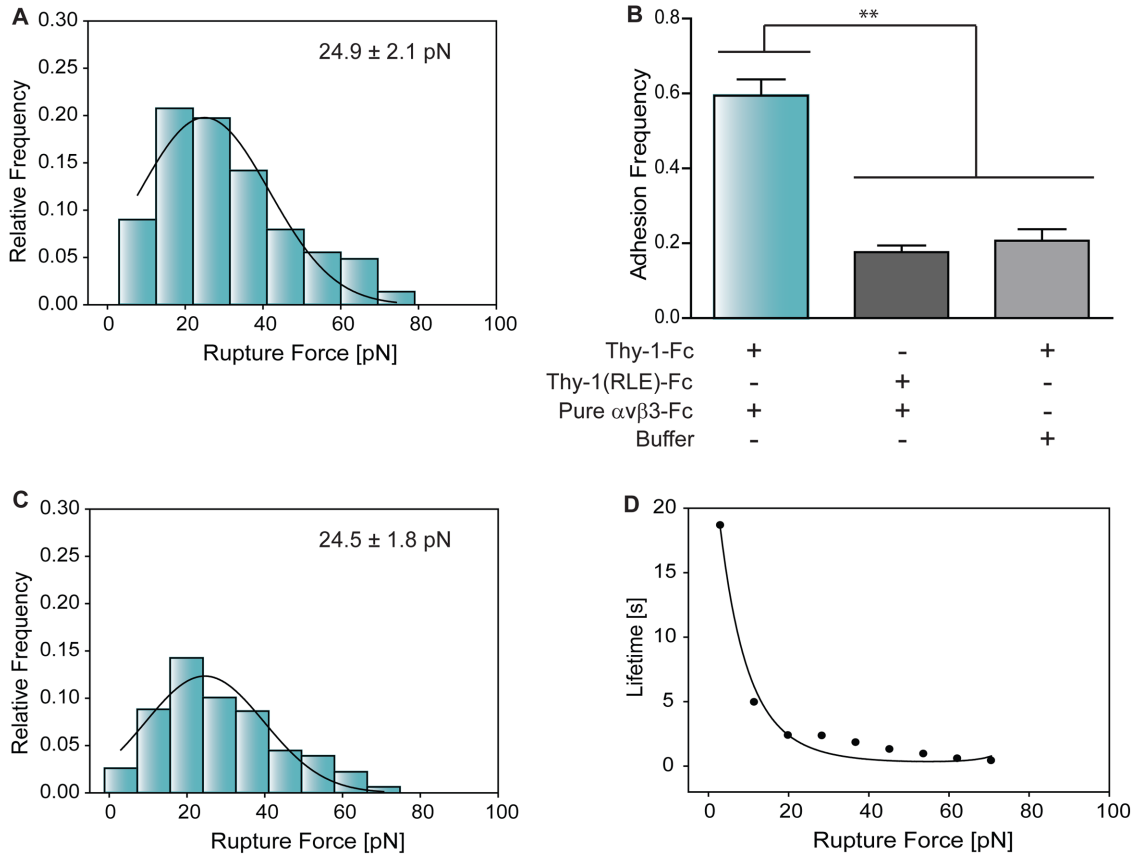

FIGURE 4: Characterization of rupture force distribution, adhesion frequency, and binding parameters between Thy-1-Fc and pure αvβ3-Fc integrin. (A) Rupture force histogram of the interaction between Thy-1-Fc and the purified αvβ3-Fc fusion protein. (B) Adhesion frequencies were evaluated for Thy-1-Fc/pure αvβ3-Fc protein, Thy-1(RLE)-Fc/pure αvβ3-Fc, and Thy-1-Fc/ HEPES buffer conditions. All adhesion frequencies were assessed by measuring the number of total binding events in at least 60 approach-retraction cycles per five pairs of new beads. (C) Rupture force histogram of Thy-1-Fc and purified αvβ3-Fc interactions resulting after applying the mathematical strategy to filter rupture forces due to nonspecific binding. The solid lines in A and C correspond to the Gauss function used to approximate the distribution of rupture forces and to characterize peak rupture force. Histograms were obtained at a loading rate of 10 pN/s and at least 300 binding events per five pairs of new beads. (D) Force-dependent lifetime for the Thy-1-Fc/pure αvβ3-Fc integrin interaction, estimated from each bin in C, using the Dudko-Hummer-Szabo model (Eq. 1). Solid line in D corresponds to the fitted equation 2 ($\upsilon = 0.5$).

indicating interaction specificity with integrin-binding molecules (Figure S5). As for the nonpurified protein, the concentration of the pure αvβ3-Fc was estimated by a semiquantitative Western blotting assay (Supplemental Figure S4D) and validated using the bicinchoninic acid assay. The determined concentration was ~130 nM. To ensure correct comparisons with the parameters estimated for the nonpurified fusion protein, pure αvβ3-Fc was diluted 10^6-fold. The peak rupture force obtained between Thy-1-Fc and the diluted pure αvβ3-Fc was 24.9 ± 2.1 pN (Figure 4A).

To test the binding specificity between Thy-1-Fc and the pure αvβ3-Fc integrin, thereby confirming whether the use of a purified protein eliminated nonspecific binding events, a range of adhesion frequency measurements were carried out. A higher adhesion frequency was observed for the pure αvβ3-Fc protein with Thy-1-Fc than with the mutant Thy-1(RLE)-Fc (Figure 4B), indicating that this purified protein can still directly interact with the RLD motif in Thy-1-Fc. Considering that Thy-1-Fc nonspecifically interacted with the buffer-treated beads, the adhesion frequency was evaluated between Thy-1-Fc and beads preincubated with the HEPES buffer. As expected, a similar adhesion frequency was observed as compared with the control Thy-1(RLE)-Fc/pure αvβ3-Fc condition (Figure 4B). Moreover, similar rupture force distribution profiles were observed for both the Thy-1(RLE)-Fc/pure αvβ3-Fc and Thy-1-Fc/buffer conditions (Supplemental Figure S3, C and D). This similarity suggests the presence of comparable nonspecific binding events even when both proteins are pure. Considering that nonspecific events represent 20% of all events, and to correctly determine the binding parameters between Thy-1-Fc/pure αvβ3-Fc, the developed mathematical method was applied to correct rupture forces from nonspecific interactions, resulting in a peak force of 24.5 ± 1.8 pN (Figure 4C).

The force-dependent lifetime data τ(F) obtained using the DHS model are shown in Figure 4D. The lifetime data were fitted by applying the nonlinear DHS model (Eq. 2; see *Materials and Methods*), thus characterizing the energy landscape of the dissociation process between Thy-1-Fc and the pure αvβ3-Fc integrin. The values obtained at zero force were as follows: binding lifetime ($\tau^0 = 27.25 \pm 7.70$ s), off-rate constant ($k_{off}^0 = 0.036 \pm 0.010$ s^{-1}), distance to the transition state ($\Delta x^{\ddagger} = 0.54 \pm 0.16$ nm), and free energy of activation ($\Delta G^{\ddagger} = 6.16 \pm 0.55$ k_BT). Importantly, these results are very similar to

	Lifetime (τ^0)	Off-rate (k_{off}^0)	Distance to transition state ($\Delta x^{\ddagger}$)	Free energy of activation ($\Delta G^{\ddagger}$)
Nonpurified αvβ3-Fc	19.30 ± 1.34 s	0.051 ± 0.003 s^{-1}	0.50 ± 0.05 nm	5.54 ± 0.47 *k*B*T*
Pure αvβ3-Fc	27.25 ± 7.70 s	0.036 ± 0.010 s^{-1}	0.54 ± 0.16 nm	6.16 ± 0.55 *k*B*T*

TABLE 1: Comparison of kinetic and thermodynamic parameters in the absence of force.

those obtained with nonpurified αvβ3-Fc in the crude supernatant after applying the mathematical model designed to eliminate nonspecific interactions (see Table 1).

Taken together, our findings indicate that the developed mathematical approach allows for precisely characterizing the effects of mechanical forces on the Thy-1-Fc/αvβ3-Fc interaction, even when one of the proteins is unavailable in the purified state.

DISCUSSION

In this study, we characterized for the first time how force regulates interaction dissociations between the glycoprotein Thy-1 and the αvβ3 integrin, proteins that mediate cell–cell adhesion (Saalbach *et al.*, 2005; Herrera-Molina *et al.*, 2013), including bidirectional neuron-to-astrocyte communication (Hermosilla *et al.*, 2008; Herrera-Molina *et al.*, 2012; Alvarez *et al.*, 2016; Maldonado *et al.*, 2016). Direct force measurement results of the interaction between the αvβ3 integrin and Thy-1 were obtained using optical tweezers. This force-transducer technique (Ashkin, 1997; Smith *et al.*, 2003) has been employed to research different bimolecular interactions, such as those between αIIbβ3 integrin/fibrinogen (Litvinov *et al.*, 2005, 2011), P- and L-selectins/PSGL-1 (Rinko *et al.*, 2004), and αvβ3 integrin/osteopontin (Litvinov *et al.*, 2003).

Molecular force spectroscopy is the experimental approach of choice for studying how mechanical forces regulate bimolecular interactions (Fiore, Ju, *et al.*, 2014; Li *et al.*, 2003), which has been also used to study intact cells and purified proteins (Zhang *et al.*, 2004; Litvinov *et al.*, 2005; Sun *et al.*, 2005). This technique is highly sensitive, and purified proteins are desirable to reduce the possibility of nonspecific interactions. However, the purification of a protein could represent a limiting factor. In our own previous attempt to purify the αvβ3-Fc fusion protein, the final purified product was a nonfunctional integrin (Hermosilla *et al.*, 2008). To overcome this limitation, we designed an experimental and mathematical strategy that allowed us to perform the present study with a nonpurified αvβ3-Fc fusion protein. For this, supernatants containing the αvβ3-Fc protein were incubated with protein G-coated beads to separate the integrin from other molecules, as is commonly achieved in pull-down assays. Surprisingly, even when protein G specifically interacts with the Fc fragment (Kato *et al.*, 1995), rupture forces due to nonspecific interactions were detected between Thy-1 and the other soluble molecules. Moreover, Thy-1-Fc interacted nonspecifically with the beads themselves. Interestingly, the strength determined for these nonspecific interactions reached values of ~10 pN (i.e., peak of rupture forces), which are in line with previous reports for nonspecific protein–protein interactions (Weisel *et al.*, 2003; Litvinov *et al.*, 2005). This rupture force peak differed from that obtained with the supernatants containing the αvβ3-Fc protein (~25 pN); however, in the lower force range, the nonspecific interactions partially overlapped the specific Thy-1/αvβ3 interaction. To overcome this issue, a mathematical algorithm was developed and used to correct the nonspecific rupture forces and, consequently, obtain an accurate estimation of the dissociation rupture forces of specific Thy-1-Fc/αvβ3-Fc interactions.

To confirm the results obtained with the nonpurified αvβ3-Fc integrin, and to validate the employed mathematical approximation, pure and stable αvβ3-Fc protein was obtained as reported for α5β1-Fc (Coe *et al.*, 2001). The purified αvβ3-Fc bound to ligands containing an integrin-binding site (e.g., fibronectin and vitronectin) as expected (Charo *et al.*, 1990), corroborating the notion that mutations in the Fc fragments did not affect the ability of the αvβ3-Fc integrin to interact with corresponding ligands, such as Thy-1. Importantly, the unbinding parameters of the Thy-1-Fc/pure αvβ3-Fc interaction were highly comparable to those obtained with nonpurified αvβ3-Fc in the crude supernatants after filtering nonspecific interactions. This observation demonstrates that our approach permits characterizing how protein–protein interactions respond to mechanical forces, even when one of the molecules involved is not available in the purified state.

In assessing the nonpurified αvβ3-Fc protein, rupture forces resulting from single-molecule interactions were corroborated using several criteria. For instance, the obtained histograms showed forces resulting only from single-step bond ruptures (force-trap position graphs, Figure 1, J and K). While multiple binding events are represented by a series of peaks in rupture force histograms, single binding events are characterized by a unique peak (Weisel *et al.*, 2003; Litvinov *et al.*, 2005). The two-peak rupture forces detected when nondiluted supernatants containing αvβ3-Fc protein were evaluated (Figure 1B) suggest the presence of multiple binding events. However, a single peak at ~25 pN appeared when the integrin was diluted (Figure 1, D, F, and H), which would be representative of single-binding events. Furthermore, the peak of rupture forces for single-binding events should not be modified by changes in the surface density of the interacting proteins (Zhu *et al.*, 2002; Litvinov *et al.*, 2005). Accordingly, a peak value of ~25 pN was detected for each dilution of the supernatant containing the αvβ3-Fc protein. In contrast, variations in surface density can change the adhesion frequency between proteins (Litvinov *et al.*, 2005). In the current assessments, a tendency towards decreased frequency values was detected on reducing the αvβ3-Fc concentration. However, a significant decrease in the adhesion frequency value was observed only when the integrin concentration was diluted to the attomolar level (i.e., 10^9 dilution).

Bond strength is the most probable bond rupture force and can be estimated from rupture–force distribution histograms (Evans and Ritchie, 1997). In this study, a bond strength of ~25 pN was determined for Thy-1/αvβ3. The peak rupture force for adhesion proteins are characteristic of each ligand–receptor pair and range from 20 to 150 pN (Weisel *et al.*, 2003). However, it is important to note that for noncovalent interactions, bond strength also depends on the rate at which force is applied (force loading rate) (Evans and Ritchie, 1997; Rico *et al.*, 2007). Common pulling rates used in single-molecule experiments are in the range of 10^2–10^4 nm/s (Roca-Cusachs, Iskratsch, and Sheetz, 2012). Here, force-ramp assays were performed under similar conditions (i.e., constant rate of 100 nm/s), and considering the stiffness of the system (spring constant of 0.1 pN/nm), the loading rate value would be 10 pN/s (pulling rate × spring constant)

(Dudko *et al.*, 2008). By comparison, the bond strength for the interaction between fibrinogen and αIIbβ3 is ~50 pN using a pulling rate of 160 nm/s (Agnihotri *et al.*, 2009), which suggests a stronger interaction than for Thy-1/αvβ3 integrin binding. In other studies, a lower bond strength (9.2 ± 4.4 pN), as compared with the present Thy-1/αvβ3 interaction, has been reported for actin/myosin binding using a loading rate of 12 pN/s (Nishizaka *et al.*, 2000). Interestingly, results obtained by atomic force microscopy demonstrated that the interaction between the αvβ3 integrin and GRGDSP peptide has a bond strength of 42 ± 4 pN at a force loading rate of 30,000 pN/s (Lehenkari and Horton, 1999). Considering that the Thy-1/αvβ3 interaction also depends on the RGD-like integrin-binding domain (RLD), the result obtained with a fast loading rate (30,000 pN/s) suggests that force loading rate increases greater than three orders of magnitude only modify the bond strength found for the Thy-1/αvβ3 interaction by approximately twofold. Bonds that are almost insensitive to stress rates are known as "persistent bonds" and have been reported for the force responses of the interaction between the intracellular cell adhesion molecule-1 (ICAM-1) and the αLβ2 integrin (Evans and Calderwood, 2007; Evans *et al.*, 2010). In this context, we found that in the range of 5 and 100 pN/s, the bond strength for Thy-1/αvβ3 interaction is almost not affected by loading rates (Supplemental Figure S6A). Importantly, current measurements were taken using a force loading rate within the physiological range (Yamazaki *et al.*, 2002; Li *et al.*, 2003), suggesting that the bond strength observed for Thy-1/αvβ3 integrin interactions is likely representative of that existing in the CNS. Despite that bond strength depends on the rate at which force is applied, it is important to note that according to the DHS model, lifetime data obtained at different loading rates (i.e., at different pulling rate) must collapse onto a single-master curve that describes the force-dependent lifetimes (Dudko *et al.*, 2008), prediction that was observed with loading rates up to 100 pN/s (Supplemental Figure S6B). In fact, the low loading rate (10 pN/s) curve obtained was maintained at a higher loading rate (50 and 100 pN/s). Consequently, the unbinding parameters calculated for Thy-1/αvβ3 integrin interaction were not modified by an increased loading rate (Supplemental Figure S6B).

Applying the DHS model (Dudko *et al.*, 2008) to the rupture force data obtained from crude supernatants and adjusted for nonspecific binding effects resulted in an estimated off-rate of ~0.051 s^{-1} for Thy-1/αvβ3. Interestingly, an off-rate of 0.012 s^{-1} has been reported for the interaction between fibronectin and high-affinity form of the α5β1 integrin (Li *et al.*, 2003), which is also involved in cellular adhesion and migration (Danen *et al.*, 2005; Morgan *et al.*, 2013). Although the off-rate values are in the same order of magnitude, the absolute values indicate that the interaction between Thy-1 and αvβ3 integrin is less stable in the absence of force than binding between fibronectin and the α5β1 integrin. Additionally, fibronectin/α5β1 integrin binding values of $\Delta x^{\ddagger} \sim 0.42$ nm have been reported (Li *et al.*, 2003), which are similar to those obtained for the Thy-1/αvβ3 interaction ($\Delta x^{\ddagger} \sim 0.5$ nm) and indicative of ruptures for similar bond types. In both cases, the reported values are probably attributable to the RGD-like tripeptide. Likewise, the DHS model has been applied to characterize unbinding parameters for the interaction between αIIbβ3 integrin and a cyclic peptide integrin antagonist, a drug used to prevent interaction of the platelet integrin αIIbβ3 with fibrinogen and blood clot formation (Dutta, Horita, *et al.*, 2013). The αIIbβ3/antagonist interaction had an off-rate of ~0.02 s^{-1}, indicating that the rate at which the dissociation between Thy-1 and αvβ3 integrin occurs is faster than that for αIIbβ3/antagonist binding. This result is to be expected given that the free energy of activation calculated for the αIIbβ3/antagonist interaction (~11.7 k_BT) is greater than the values described herein for Thy-1 and the αvβ3 integrin (~5.54 k_BT).

In the present study, force exponentially accelerated Thy-1/αvβ3 integrin dissociation, suggesting a slip bond behavior. This behavior has been described for the interaction between αIIbβ3 and fibrinogen in a force range up to 50 pN (Litvinov *et al.*, 2011). However, the catch bond phenomenon has been described most widely for integrin molecules. For instance, force prolongs bond lifetime up to 15 pN in the interaction between αLβ2 and ICAM-1 (Chen *et al.*, 2010). Interestingly, the interaction between αvβ3 integrin and fibronectin also shows a catch regime in the range of 0–20 pN (Elosegui-Artola *et al.*, 2016; Chen *et al.*, 2017), indicating differences between both Thy-1/αvβ3 and fibronectin/αvβ3 integrin interactions. Such differences have also been found for α5β1 integrin. The fibronectin/α5β1 integrin interaction shows catch bond behavior in which maximum lifetimes occur at forces of 10–30 pN (Kong *et al.*, 2009). Nevertheless, as well as for αvβ3 integrin, an ordinary slip bond behavior has been described for the interaction between Thy-1 and α5β1 integrin (Fiore, Ju, *et al.*, 2014). For α5β1 integrin, the catch bond mechanism depends on the synergy-site engagement (Friedland, Lee, and Boettiger, 2009; Sun *et al.*, 2016). Particularly in the absence of mechanical tension, the α5β1 integrin interacts with the tripeptide RGD motif present in the 10th type III module of fibronectin (FNIII10) (Aota *et al.*, 1994); however, under tensile forces, this integrin additionally engage the synergy-site in FNIII9 to form a catch bond (Friedland, Lee, and Boettiger, 2009; Kong *et al.*, 2009). In contrast to fibronectin, Thy-1 interacts either with α5β1 or αvβ3 integrin only through its RGD-like integrin-binding domain (RLD) (Hermosilla *et al.*, 2008; Herrera-Molina *et al.*, 2013; Fiore, Ju, *et al.*, 2014), which could account for the slip bond behavior. Thus, even when the catch bond mechanism for αvβ3 integrin has not been characterized yet, the differences found with fibronectin and Thy-1 could depend on the presence of synergy-site contacts for the integrins. As mentioned, Fiore and colleagues identified a slip bond behavior between Thy-1 and α5β1 integrin. However, a triphasic force dependence (slip-catch-slip) was observed for interactions with the α5β1 bound to a cell specifically expressing this integrin in the membrane instead of the purified Fc-protein. Our previous research describing the interactions between Thy-1 and the proteoglycan syndecan-4 (Avalos, Valdivia, *et al.*, 2009; Kong, Munoz, *et al.*, 2013; Alvarez *et al.*, 2016) support that Thy-1 forms a trimolecular bond with integrin and syndecan-4. This trimolecular bond displays a triphasic phenomenon termed dynamic catch, where increasing force abruptly stiffens the complex and is followed by the formation of a catch bond (Fiore, Ju, *et al.*, 2014). Our prior results further indicate that the neuronal Thy-1 and astrocytic syndecan-4 interaction is involved in neuron-to-astrocyte bidirectional communication mediated by the Thy-1/αvβ3 integrin interaction (Avalos, Valdivia, *et al.*, 2009; Kong, Munoz, *et al.*, 2013). Considering that Thy-1 interacts with syndecan-4 and αvβ3, both astrocytic molecules, and that syndecan-4 levels are upregulated in astrocytes following CNS injury (Iseki *et al.*, 2002), as is also the case for the αvβ3 integrin (Ellison *et al.*, 1999; Lagos-Cabre, Alvarez, *et al.*, 2017), the results reported by Fiore and colleagues (Fiore, Ju, *et al.*, 2014) suggest that the Thy-1/αvβ3 integrin/syndecan-4 complex may also exhibit dynamic catch bond behavior in our model system; however, whether this is indeed the case remains to be determined.

In summary, to our knowledge, our study is the first to evaluate the mechanical response of bimolecular Thy-1/αvβ3 integrin binding, providing a detailed characterization of the energy landscape for the dissociation pathway of this interaction. Importantly, we

developed a simple mathematical methodology to investigate how tensile forces tune the kinetics of protein–protein interactions at the single-molecule level. Clearly, further studies are required to fully understand the mechanical regulation of the Thy-1 and αvβ3 integrin interaction in a physiological context. Nonetheless, our research provides an initial step towards facilitating better comprehensions of how neuron and astrocyte communication processes sense and respond to mechanical forces and, consequently, how these events affect the complex behavior of these cell–cell interactions.

MATERIALS AND METHODS

Preparation of Fc-tagged fusion proteins

The recombinant proteins Thy-1-Fc wild-type and the Thy-1(RLE)-Fc mutant for the integrin-binding site were obtained and purified as previously reported (Leyton *et al.*, 2001; Hermosilla *et al.*, 2008). The αvβ3-Fc fusion protein was expressed in HEK293T cells by transient cotransfection with equal amounts (10 µg) of both αv-Fc (PS711) and β3-Fc (PS675) expression plasmids encoding for the extracellular domains of human αv and β3 integrin subunits fused to the Fc portion of the IgG1 (kindly donated by Pascal Schneider, Department of Biochemistry, University of Lausanne, Switzerland) (Schneider, 2000), using the X-treme GENE HP DNA Transfection Reagent (Roche). After 16 h of transfection, cells were grown in serum-free medium (DMEM, high glucose) for 2 d. Next, the culture serum-free supernatant containing secreted αvβ3-Fc heterodimer was centrifuged (800 rpm × 5 min), filtered (0.2 µm; Whatman), and stored at –20°C. Control supernatant was obtained by transfection of HEK293T cells with mock plasmids (pCR3.1) in serum-free medium for 2 d and recovered as indicated for αvβ3-Fc-containing supernatant.

Purification of αvβ3-Fc fusion protein

Human αvβ3-Fc integrin was purified from culture supernatants of transfected HEK293T cells via the Fc domain after mixing supernatant (3 ml) with protein-A-sepharose (500 µl; Sigma) at 4°C for 16 h. Resin with bound proteins was collected in a column and washed with Tris-buffered saline (Tris-HCl 50 mM, pH 7.5; NaCl 150 mM). Proteins were eluted with citric acid (50 mM, pH 2.7) and neutralized with Tris-HCl (1 M, pH 8.0). Eluates obtained were mixed and concentrated in ultracentrifuge tubes (Amicon 30 K). To enhance the probability of heterodimerization between αv-Fc and β3-Fc after low-pH treatment, specific mutations were introduced into the C_H3 domains of Fc fragments by oligonucleotide-directed PCR mutagenesis as described (Coe *et al.*, 2001). Specifically, in the Fc DNA of the αv-Fc subunit, the small amino acid threonine (residue 366) was changed to the large amino acid tyrosine (to create a "knob"), and in the Fc DNA of the β3-Fc subunit the large amino acid tyrosine (residue 407) was changed to a threonine (to create a "hole") (Ridgway *et al.*, 1996). Both nonpurified and pure αvβ3-Fc proteins used in this study contain the mutations in the Fc fragments.

Characterization of the αvβ3-Fc fusion protein

Nonpurified αvβ3-Fc fusion protein was detected in the supernatant of transfected HEK293T cells by Coomassie blue–stained SDS–PAGE. Eluted αvβ3-Fc integrin was characterized by Silver staining and on immunoblots under reducing and nonreducing conditions using specific anti-human IgG (Fc specific)-horseradish peroxidase (HRP) antibody (1:2000; Sigma). Semiquantitative Western blotting was performed to estimate the amount of purified αvβ3-Fc fusion protein, as well as the nonpurified αvβ3-Fc presents in supernatants. The standard curve based on signal intensity was generated using different amounts of the fusion protein of the receptor for the soluble apoptosis-inducing ligand TRAIL (TRAIL-R2-Fc) (Schneider, 2000). The functionality of αvβ3-Fc was tested using an enzyme-linked immunosorbent assay as previously described (Hermosilla *et al.*, 2008). This assay allowed evaluating the ability of both nonpurified and pure αvβ3-Fc to interact with RGD-containing ligands, including fibronectin, vitronectin, and snake venom peptides (Kis RGD-peptide) (Hermosilla *et al.*, 2008; Leyton *et al.*, 2001). As a negative control, RGE peptides were used. Integrin-ligands were immobilized in a 96-well plate (Maxisorp, Nunc). After blocking nonspecific binding sites with 1% bovine serum albumin (BSA) in phosphate-buffered saline (PBS), supernatants containing the αvβ3-Fc protein (25 µl) as well as the purified and concentrated αvβ3-Fc fusion protein (1 µl) were added to the wells, incubated, and washed, and bound Fc-tagged proteins were detected with HRP-coupled goat anti-human IgG. The chromogenic substrate 3,3 ,5,5 -tetramethylbenzidine (TMB; Thermo Scientific) was used to reveal the HRP activity. TMB solution was added to each well (100 µl) and incubated at room temperature for 30 min. Reaction was stopped with sulfuric acid (2 M, 100 µl), and absorbance was read at 450 nm in a Infinite 200 pro NanoQuant Microplate Readers (Tecan).

Depletion of αvβ3-Fc fusion protein from supernatant

Supernatant containing the αvβ3-Fc fusion protein (500 µl) was incubated with an excess of protein A-sepharose beads (50 µl) during 1 h at 4°C. The solution was then centrifuged at 2000 rpm × 5 min. This process was repeated four times, to ensure complete depletion of the fusion protein. Each supernatant and precipitate obtained was evaluated by Western blotting using anti-human IgG (Fc specific)-HRP antibody (1:2000; Sigma). After the fourth incubation/centrifugation cycle, the level of the αvβ3-Fc protein was undetectable in the precipitate (precipitate 4); thus the fourth supernatant was used in the miniTweezers experiments.

Optical tweezers setup and force measurement protocols

Molecular force spectroscopy experiments were performed with the miniTweezers instrument, which has a dual-laser beam single trap design (Smith *et al.*, 2003). The rupture forces required to dissociate protein–protein interactions are measured optically by the change in momentum of the light beams leaving the trap. This instrument is capable of force, spatial, and time resolution of 0.1 pN, 0.1–2 nm, and 10^{-4} s at 100-Hz bandwidth (Moffitt *et al.*, 2008; Neuman and Nagy, 2008). Details of the miniTweezers instrument and its operation are available on http://tweezerslab.unipr.it. All experiments were carried out in a temperature-controlled room at 25°C employing HEPES buffer (10 mM HEPES, pH 7.4, 150 mM NaCl) containing 1 mM $MgCl_2$, and using a microchamber with a glass micropipette (inner diameter <1 µm). Considering the properties of our recombinant molecules (Fc-tagged proteins: Thy-1-Fc and αvβ3-Fc), we used protein G-coated polystyrene particles (Spherotech) to attach the molecules via the Fc fragment. To study the mechanical rupture of the Thy-1-Fc/αvβ3-Fc interaction, the bead (3.1 µm) coated with αvβ3-Fc was held in the optical trap, while the bead (2.1 µm) coated with Thy-1-Fc was held on the tip of the micropipette by suction, and cycles of approaching and retraction of the beads were performed. Binding between proteins was observed after bringing the beads into close proximity by moving the optically trapped bead toward the other bead attached to the micropipette (approaching). To dissociate Thy-1-Fc/αvβ3-Fc interaction, a force-ramp assay was performed, where the optically trapped bead is moved in the opposite direction at a constant pulling rate of 100 nm/s (retraction). Considering the stiffness of the system (0.1 pN/nm), the value of the loading rate at which the dissociation was induced corresponds to

10 pN/s (pulling rate × spring constant) (Dudko *et al.*, 2008). If the protein-protein interaction occurs, then the trapped bead is displaced from the center of the optical trap and force is generated. When the force generated is greater than the force required to dissociate the binding, rupture of the interaction is observed; the force is measured directly via the deflection of the trapping laser beams by the trapped bead. The rupture force histograms were obtained with at least 300 binding events per five pairs of new beads and were normalized for the total number of approaching cycles. The bin size (*b*) was calculated using Scott's rule: $b = 3.5\sigma/(n)^{1/3}$ in which σ is the SD and *n* the number of rupture events (Scott, 1979). Adhesion frequency was calculated by measuring the total number of binding events observed in at least 50 approach–retraction cycles per five pairs of new beads.

Optical tweezers data analysis

Rupture force histograms were analyzed using the DHS model (Dudko *et al.*, 2008), which permits transforming them into force-dependent lifetimes τ(F) as follows:

$$\tau\left(F_0 + (k-1/2)\Delta F\right) = \frac{\left(h_k/2 + \sum_{i=k+1}^{N} h_i\right)\Delta F}{h_k \dot{F}\left(F_0 + (k-1/2)\Delta F\right)} \quad (1)$$

Here, a rupture force histogram contains *N* bins of width ΔF that starts at F_0 and ends at $F_N = F_0 + N\Delta F$. The number of counts in the *i*th bin is C_i, resulting in height $h_i = C_i/(N_{tot}\Delta F)$, where N_{tot} is the total number of counts; $k = 1,2,\ldots$

After applying Eq. 1, data points of the τ(f)-versus-*F* plot were obtained. The DHS model interpreted the force-dependence lifetime assuming that dissociation of protein–protein binding can be described as an escape from a deep one-dimensional free energy well (Dudko *et al.*, 2008). Therefore, with the following nonlinear DHS model, the energy landscape and kinetic parameters of the dissociation process at a constant loading rate were characterized as follows:

$$\tau(F) = \tau_0\left(1 - \frac{vFx^{\ddagger}}{\Delta G^{\ddagger}}\right)^{1-1/v} e^{-\beta\Delta G^{\ddagger}\left[1-\left(1-vFx^{\ddagger}/\Delta G^{\ddagger}\right)^{1/v}\right]} \quad (2)$$

In this expression, *F* is the externally applied force and $\beta = (k_B T)^{-1}$ is the inverse thermal energy, τ_0 is the lifetime of the interaction at zero force [inversely related to off-rate constant, (τ_0^{-1})], $\Delta x^{\ddagger}$ is the distance to the transition state, and $\Delta G^{\ddagger}$ is the apparent free energy of activation, describing the energy barrier that must be overcome to dissociate the interaction between Thy-1-Fc and αvβ3-Fc in the absence of force. The scaling factor *v* describes the shape of the underlying free energy landscape. The variable $v = 1/2$ corresponds to a harmonic well with a cusplike barrier, while $v = 2/3$ corresponds to a potential that contains linear and cubic terms. For $v = 1$, Bell's formula is recovered (Bell, 1978). Both *v* values 1/2 and 2/3 fitted well to our data.

Mathematical model to correct rupture force due to nonspecific binding events.

Considering only the cases in which interactions actually occur (these cases are those giving relevant information), two possible outcomes exist: Thy-1-Fc interacts in a specific manner with the αvβ3-Fc integrin (event *AB*) or Thy-1-Fc interacts in a nonspecific manner with either other proteins present in the integrin-containing supernatant or the surface of the bead (event $\overline{AB}$). These events are assumed to be mutually exclusive due to the single-molecule conditions of the experiments, which prohibit both events from occurring simultaneously. The presence of single binding events is supported by the fast, single cooperative rips at which rupture events occurred (see Figure 1J), as opposed to multiple-ripping patterns observed when the rupture of multiple bonds occurs. Applying the law of total probability, the probability of obtaining a rupture force between *F* and *F* + *dF*, *P*(*F*) will be given by the following:

$$P(F) = P\left(F\middle|AB\right)P(AB) + P\left(F\middle|\overline{AB}\right)P\left(\overline{AB}\right) \quad (3)$$

Here $P\left(F\middle|AB\right)$ and $P\left(F\middle|\overline{AB}\right)$ are the normalized rupture force histograms for the conditions studied between Thy-1-Fc/αvβ3-Fc-containing supernatant and Thy-1-Fc/supernatant from mock-transfected cells, respectively. $P(AB)$ defines the probability of detecting a specific interaction (Thy-1-Fc/αvβ3-Fc; Figure 3B), while $P\left(\overline{AB}\right) \equiv \left(1 - P(AB)\right)$ indicates the probability of being a nonspecific interaction (Thy-1-Fc/other proteins or Thy-1-Fc/bead; Figure 3, A and B).

Using Bayes's theorem (Bois, 2013), it is possible to obtain useful expression for $P\left(AB\middle|F\right)$ and $P\left(\overline{AB}\middle|F\right)$ as follows:

$$P\left(AB\middle|F\right) = P\left(F\middle|AB\right)\frac{P(AB)}{P(F)} \quad (4)$$

$$P\left(\overline{AB}\middle|F\right) = P\left(F\middle|\overline{AB}\right)\frac{P\left(\overline{AB}\right)}{P(F)} \quad (5)$$

In these expressions, $P\left(AB\middle|F\right)$ and $P\left(\overline{AB}\middle|F\right)$ are the probabilities to find interactions between Thy-1-Fc and the αvβ3-Fc integrin or other proteins given the rupture force was between *F* + *DF*, respectively. These three relationships (Eqs. 3, 4, and 5) allowed us to obtain the specific interaction events between Thy-1 and the αvβ3 integrin by measuring the nonspecific interactions and the mixed (specific + nonspecific) interactions.

In practical terms, if we define $h(F) \equiv P(F)$, the rupture force histogram for the mixed interactions (i.e., condition studied between Thy-1-Fc/supernatant-containing αvβ3-Fc where both specific and nonspecific interactions are detected); $f_{AB}(F) \equiv P\left(F\middle|AB\right)$, the rupture force histogram for the specific Thy-1/αvβ3-Fc interactions; $f_{\overline{AB}}(F) \equiv P\left(F\middle|\overline{AB}\right)$, the rupture force histogram for the conditions between Thy-1-Fc/supernatant from mock-transfected cells (without αvβ3-Fc); and $\alpha \equiv P(AB)$, the mixing parameter that defines the probability to detect a specific interaction (Thy-1-Fc/αvβ3-Fc), the equations are as follows:

$$h(F) = \alpha f_{AB}(F) + (1-\alpha) f_{\overline{AB}}(F) \quad (6)$$

$$P\left(AB\middle|F\right) = \alpha\frac{f_{AB}(F)}{h(F)} \quad (7)$$

$$P\left(\overline{AB}\middle|F\right) = (1-\alpha)\frac{f_{AB}(F)}{h(F)} \quad (8)$$

These expressions represent a direct method of obtaining the specific interactions between Thy-1-Fc and the αvβ3-Fc integrin in the nonpurified state, using rupture force data from the Thy-1-Fc/αvβ3-Fc supernatant (specific + nonspecific binding events) and the Thy-1-Fc/mock plasmid supernatant (nonspecific binding events) conditions. The equations are derived from basic rules of statistics and correspond to a valid representation, as long as the nonspecific interactions are independent of αvβ3-Fc integrin concentration (i.e., the probability of nonspecific interactions do not change in the presence of the αvβ3-Fc fusion protein). The validity of the equations considers the following assumptions: 1) the αvβ3-Fc

protein does not compete with the nonspecific binding events mediated by Thy-1-Fc, 2) the αvβ3-Fc protein does not interact with other proteins present in the supernatant, and 3) the interactions between Thy1-Fc/αvβ3-Fc are of lower affinity than those nonspecific interactions mediated by Thy-1-Fc (Thy-1-Fc/other proteins or Thy-1-Fc/bead). Under these assumptions, the addition of the αvβ3-Fc integrin could be treated as a small perturbation to the system. Nevertheless, most likely the Thy-1/nonspecific interactions will change with the addition of αvβ3 integrin to the system, since it is clear that the αvβ3 integrin interacts with a high-affinity with its ligands (Xiao and Truskey, 1996). In real conditions, then, the αvβ3-Fc will compete with the nonspecific interactions; however, this competition will mainly affect the nonspecific binding events of lower affinity represented by the low force values in the histograms (see Figure 1, C, E, G, and I). Thus, here, with the assumptions made for our mathematical model, minor changes on the rupture force distribution caused by the competition of specific and nonspecific binding are expected to affect lower rupture force values only.

A step-by-step procedure to obtain the filtered histograms using these expressions is given in the Supplemental Material.

Statistical analysis

Data are expressed as mean ± SEM of three independent experiments. Results were analyzed by nonparametric Mann–Whitney analysis to compare two groups. Statistical significance was set at $p < 0.05$.

ACKNOWLEDGMENTS

We acknowledge financial support of the following grants: Comisión Nacional de Investigación Científica y Tecnológica (CONICYT) #21130008 (F.B.B.), Fondo Nacional de Desarrollo Científico y Tecnológico (FONDECYT) #1150744 (L.L.), #1130250 (A.F.G.Q.), #1170925 (A.F.G.Q.), #11130263 (C.A.M.W.); CONICYT-Natural Environment Research Council (NERC) #PCI-PII20150073 (C.A.M.W.); CONICYT-Fondo de Financiamiento de Centros de Investigación en Áreas Prioritarias (FONDAP) #15130011 (A.F.G.Q. and L.L.). We also acknowledge Steven B. Smith from Steven B. Smith Engineering for helping in miniTweezers construction.

REFERENCES

Boldface denotes co–first authors.

Agnihotri A, Soman P, Siedlecki CA (2009). AFM measurements of interactions between the platelet integrin receptor GPIIbIIIa and fibrinogen. Colloids Surf B Biointerf 71, 138–147.

Alvarez A, Lagos-Cabre R, Kong M, Cardenas A, Burgos-Bravo F, Schneider P, Quest AF, Leyton L (2016). Integrin-mediated transactivation of P2X7R via hemichannel-dependent ATP release stimulates astrocyte migration. Biochim Biophys Acta 1863, 2175–2188.

Ananthakrishnan R, Ehrlicher A (2007). The forces behind cell movement. Int J Biol Sci 3, 303–317.

Aota S, Nomizu M, Yamada KM (1994). The short amino acid sequence Pro-His-Ser- Arg-Asn in human fibronectin enhances cell-adhesive function. J Biol Chem 269, 24756–24761.

Ashkin A (1997). Optical trapping and manipulation of neutral particles using lasers. Proc Natl Acad Sci USA 94, 4853–4860.

Avalos AM, Valdivia AD, Munoz N, Herrera-Molina R, Tapia JC, Lavandero S, Chiong M, Burridge K, Schneider P, Quest AF, *et al.* (2009). Neuronal Thy-1 induces astrocyte adhesion by engaging syndecan-4 in a cooperative interaction with alphavbeta3 integrin that activates PKCalpha and RhoA. J Cell Sci 122, 3462–3471.

Bell GI (1978). Models for the specific adhesion of cells to cells. Science 200, 618–627.

Benarroch EE (2005). Neuron-astrocyte interactions: partnership for normal function and disease in the central nervous system. Mayo Clin Proc 80, 1326–1338.

Bois FY (2013). Bayesian inference. Methods Mol Biol 930, 597–636.

Bushong EA, Martone ME, Jones YZ, Ellisman MH (2002). Protoplasmic astrocytes in CA1 stratum radiatum occupy separate anatomical domains. J Neurosci 22, 183–192.

Coe AP, Askari JA, Kline AD, Robinson MK, Kirby H, Stephens PE, Humphries MJ (2001). Generation of a minimal alpha5beta1 integrin-Fc fragment. J Biol Chem 276, 35854–35866.

Charo IF, Nannizzi L, Smith JW, Cheresh DA (1990). The vitronectin receptor alpha v beta 3 binds fibronectin and acts in concert with alpha 5 beta 1 in promoting cellular attachment and spreading on fibronectin. J Cell Biol 111, 2795–2800.

Chen W, Lou J, Zhu C (2010). Forcing switch from short- to intermediate- and long- lived states of the alphaA domain generates LFA-1/ICAM-1 catch bonds. J Biol Chem 285, 35967–35978.

Chen Y, Lee H, Tong H, Schwartz M, Zhu C (2017). Force regulated conformational change of integrin alphaVbeta3. Matrix Biol 60–61, 70–85.

Danen EH, van Rheenen J, Franken W, Huveneers S, Sonneveld P, Jalink K, Sonnenberg A (2005). Integrins control motile strategy through a Rho-cofilin pathway. J Cell Biol 169, 515–526.

Dembo M, Torney DC, Saxman K, Hammer D (1988). The reaction-limited kinetics of membrane-to-surface adhesion and detachment. Proc R Soc Lond B Biol Sci 234, 55–83.

Dudko OK, Hummer G, Szabo A (2008). Theory, analysis, and interpretation of single- molecule force spectroscopy experiments. Proc Natl Acad Sci USA 105, 15755–15760.

Dutta S, Horita DA, Hantgan RR, Guthold M (2013). Probing alphaiibbeta3: ligand interactions by dynamic force spectroscopy and surface plasmon resonance. Nano Life 3, 1340005.

Elosegui-Artola A, Oria R, Chen Y, Kosmalska A, Perez-Gonzalez C, Castro N, Zhu C, Trepat X, Roca-Cusachs P (2016). Mechanical regulation of a molecular clutch defines force transmission and transduction in response to matrix rigidity. Nat Cell Biol 18, 540–548.

Ellison JA, Barone FC, Feuerstein GZ (1999). Matrix remodeling after stroke. De novo expression of matrix proteins and integrin receptors. Ann NY Acad Sci 890, 204–222.

Evans E, Kinoshita K, Simon S, Leung A (2010). Long-lived, high-strength states of ICAM-1 bonds to beta2 integrin, I: lifetimes of bonds to recombinant alphaLbeta2 under force. Biophys J 98, 1458–1466.

Evans E, Ritchie K (1997). Dynamic strength of molecular adhesion bonds. Biophys J 72, 1541–1555.

Evans EA, Calderwood DA (2007). Forces and bond dynamics in cell adhesion. Science 316, 1148–1153.

Fiore VF, Ju L, Chen Y, Zhu C, Barker TH (2014). Dynamic catch of a Thy-1-alpha5beta1+syndecan-4 trimolecular complex. Nat Commun 5, 4886.

Fournier MF, Sauser R, Ambrosi D, Meister JJ, Verkhovsky AB (2010). Force transmission in migrating cells. J Cell Biol 188, 287–297.

Friedland JC, Lee MH, Boettiger D (2009). Mechanically activated integrin switch controls alpha5beta1 function. Science 323, 642–644.

Govek EE, Newey SE, Van Aelst L (2005). The role of the Rho GTPases in neuronal development. Genes Dev 19, 1–49.

Gumbiner BM (1996). Cell adhesion: the molecular basis of tissue architecture and morphogenesis. Cell 84, 345–357.

Halassa MM, Fellin T, Takano H, Dong JH, Haydon PG (2007). Synaptic islands defined by the territory of a single astrocyte. J Neurosci 27, 6473–6477.

Hermosilla T, Munoz D, Herrera-Molina R, Valdivia A, Munoz N, Nham SU, Schneider P, Burridge K, Quest AF, Leyton L (2008). Direct Thy-1/alphaV-beta3 integrin interaction mediates neuron to astrocyte communication. Biochim Biophys Acta 1783, 1111–1120.

Herrera-Molina R, Frischknecht R, Maldonado H, Seidenbecher CI, Gundelfinger ED, Hetz C, Aylwin Mde L, Schneider P, Quest AF, Leyton L (2012). Astrocytic alphaVbeta3 integrin inhibits neurite outgrowth and promotes retraction of neuronal processes by clustering Thy-1. PLoS One 7, e34295.

Herrera-Molina R, Valdivia A, Kong M, Alvarez A, Cardenas A, Quest AF, Leyton L (2013). Thy-1-interacting molecules and cellular signaling in cis and trans. Int Rev Cell Mol Biol 305, 163–216.

Iseki K, Hagino S, Mori T, Zhang Y, Yokoya S, Takaki H, Tase C, Murakawa M, Wanaka A (2002). Increased syndecan expression by pleiotrophin and FGF receptor-expressing astrocytes in injured brain tissue. Glia 39, 1–9.

Kato K, Lian LY, Barsukov IL, Derrick JP, Kim H, Tanaka R, Yoshino A, Shiraishi M, Shimada I, Arata Y, *et al.* (1995). Model for the complex between protein G and an antibody Fc fragment in solution. Structure 3, 79–85.

Khalili AA, Ahmad MR (2015). A review of cell adhesion studies for biomedical and biological applications. Int J Mol Sci 16, 18149–18184.

Kong F, Garcia AJ, Mould AP, Humphries MJ, Zhu C (2009). Demonstration of catch bonds between an integrin and its ligand. J Cell Biol 185, 1275–1284.

Kong M, Munoz N, Valdivia A, Alvarez A, Herrera-Molina R, Cardenas A, Schneider P, Burridge K, Quest AF, Leyton L (2013). Thy-1-mediated cell-cell contact induces astrocyte migration through the engagement of alphaVbeta3 integrin and syndecan-4. Biochim Biophys Acta 1833, 1409–1420.

Kranenburg O, Poland M, Gebbink M, Oomen L, Moolenaar WH (1997). Dissociation of LPA-induced cytoskeletal contraction from stress fiber formation by differential localization of RhoA. J Cell Sci 110(Pt 19), 2417–2427.

Lagos-Cabre R, Alvarez A, Kong M, Burgos-Bravo F, Cardenas A, Rojas-Mancilla E, Perez-Nunez R, Herrera-Molina R, Rojas F, Schneider P, *et al.* (2017). alphaVbeta3 Integrin regulates astrocyte reactivity. J Neuroinflammation 14, 194.

Lehenkari PP, Horton MA (1999). Single integrin molecule adhesion forces in intact cells measured by atomic force microscopy. Biochem Biophys Res Commun 259, 645–650.

Leyton L, Hagood JS (2014). Thy-1 modulates neurological cell-cell and cell-matrix interactions through multiple molecular interactions. Adv Neurobiol 8, 3–20.

Leyton L, Schneider P, Labra CV, Ruegg C, Hetz CA, Quest AF, Bron C (2001). Thy- 1 binds to integrin beta(3) on astrocytes and triggers formation of focal contact sites. Curr Biol 11, 1028–1038.

Li F, Redick SD, Erickson HP, Moy VT (2003). Force measurements of the alpha5beta1 integrin-fibronectin interaction. Biophys J 84, 1252–1262.

Litvinov RI, Barsegov V, Schissler AJ, Fisher AR, Bennett JS, Weisel JW, Shuman H (2011). Dissociation of bimolecular alphaIIbbeta3-fibrinogen complex under a constant tensile force. Biophys J 100, 165–173.

Litvinov RI, Bennett JS, Weisel JW, Shuman H (2005). Multi-step fibrinogen binding to the integrin (alpha)IIb(beta)3 detected using force spectroscopy. Biophys J 89, 2824–2834.

Litvinov RI, Vilaire G, Shuman H, Bennett JS, Weisel JW (2003). Quantitative analysis of platelet alpha v beta 3 binding to osteopontin using laser tweezers. J Biol Chem 278, 51285–51290.

Liu B, Chen W, Zhu C (2015). Molecular force spectroscopy on cells. Annu Rev Phys Chem 66, 427–451.

Maldonado H, Calderon C, Burgos-Bravo F, Kobler O, Zuschratter W, Ramirez O, Hartel S, Schneider P, Quest AF, Herrera-Molina R, *et al.* (2016). Astrocyte-to-neuron communication through integrin-engaged Thy-1/CBP/Csk/Src complex triggers neurite retraction via the RhoA/ROCK pathway. Biochim Biophys Acta 1864, 243–254.

Moffitt JR, Chemla YR, Smith SB, Bustamante C (2008). Recent advances in optical tweezers. Annu Rev Biochem 77, 205–228.

Morgan MR, Hamidi H, Bass MD, Warwood S, Ballestrem C, Humphries MJ (2013). Syndecan-4 phosphorylation is a control point for integrin recycling. Dev Cell 24, 472–485.

Neuman KC, Nagy A (2008). Single-molecule force spectroscopy: optical tweezers, magnetic tweezers and atomic force microscopy. Nat Methods 5, 491–505.

Nishizaka T, Seo R, Tadakuma H, Kinosita K Jr, Ishiwata S (2000). Characterization of single actomyosin rigor bonds: load dependence of lifetime and mechanical properties. Biophys J 79, 962–974.

Pollard TD, Borisy GG (2003). Cellular motility driven by assembly and disassembly of actin filaments. Cell 112, 453–465.

Rakshit S, Sivasankar S (2014). Biomechanics of cell adhesion: how force regulates the lifetime of adhesive bonds at the single molecule level. Phys Chem Chem Phys 16, 2211–2223.

Rico F, Roca-Cusachs P, Sunyer R, Farre R, Navajas D (2007). Cell dynamic adhesion and elastic properties probed with cylindrical atomic force microscopy cantilever tips. J Mol Recognit 20, 459–466.

Ridgway JB, Presta LG, Carter P (1996). "Knobs-into-holes" engineering of antibody CH3 domains for heavy chain heterodimerization. Protein Eng 9, 617–621.

Rinko LJ, Lawrence MB, Guilford WH (2004). The molecular mechanics of P- and L- selectin lectin domains binding to PSGL-1. Biophys J 86, 544–554.

Robert P, Benoliel AM, Pierres A, Bongrand P (2007). What is the biological relevance of the specific bond properties revealed by single-molecule studies? J Mol Recognit 20, 432–447.

Roca-Cusachs P, Iskratsch T, Sheetz MP (2012). Finding the weakest link: exploring integrin-mediated mechanical molecular pathways. J Cell Sci 125, 3025–3038.

Saalbach A, Wetzel A, Haustein UF, Sticherling M, Simon JC, Anderegg U (2005). Interaction of human Thy-1 (CD 90) with the integrin alphavbeta3 (CD51/CD61): an important mechanism mediating melanoma cell adhesion to activated endothelium. Oncogene 24, 4710–4720.

Schneider P (2000). Production of recombinant TRAIL and TRAIL receptor: Fc chimeric proteins. Methods Enzymol 322, 325–345.

Scott DW (1979). On optimal and data-based histograms. Biometrika 66, 605–610.

Smith SB, Cui Y, Bustamante C (2003). Optical-trap force transducer that operates by direct measurement of light momentum. Methods Enzymol 361, 134–162.

Sofroniew MV, Vinters HV (2010). Astrocytes: biology and pathology. Acta Neuropathol 119, 7–35.

Stangner T, Wagner C, Singer D, Angioletti-Uberti S, Gutsche C, Dzubiella J, Hoffmann R, Kremer F (2013). Determining the specificity of monoclonal antibody HPT- 101 to tau-peptides with optical tweezers. ACS Nano 7, 11388–11396.

Strunz T, Oroszlan K, Schumakovitch I, Guntherodt H, Hegner M (2000). Model energy landscapes and the force-induced dissociation of ligand-receptor bonds. Biophys J 79, 1206–1212.

Sun Z, Guo SS, Fassler R (2016). Integrin-mediated mechanotransduction. J Cell Biol 215, 445–456.

Sun Z, Martinez-Lemus LA, Trache A, Trzeciakowski JP, Davis GE, Pohl U, Meininger GA (2005). Mechanical properties of the interaction between fibronectin and alpha5beta1-integrin on vascular smooth muscle cells studied using atomic force microscopy. Am J Physiol Heart Circ Physiol 289, H2526–H2535.

Weisel JW, Shuman H, Litvinov RI (2003). Protein-protein unbinding induced by force: single-molecule studies. Curr Opin Struct Biol 13, 227–235.

Xiao Y, Truskey GA (1996). Effect of receptor-ligand affinity on the strength of endothelial cell adhesion. Biophys J 71, 2869–2884.

Yamazaki M, Furuike S, Ito T (2002). Mechanical response of single filamin A (ABP- 280) molecules and its role in the actin cytoskeleton. J Muscle Res Cell Motil 23, 525–534.

Yuan C, Chen A, Kolb P, Moy VT (2000). Energy landscape of streptavidin-biotin complexes measured by atomic force microscopy. Biochemistry 39, 10219–10223.

Zhang X, Craig SE, Kirby H, Humphries MJ, Moy VT (2004). Molecular basis for the dynamic strength of the integrin alpha4beta1/VCAM-1 interaction. Biophys J 87, 3470–3478.

Zhu C (2014). Mechanochemitry: a molecular biomechanics view of mechanosensing. Ann Biomed Eng 42, 388–404.

Zhu C, Long M, Chesla SE, Bongrand P (2002). Measuring receptor/ligand interaction at the single-bond level: experimental and interpretative issues. Ann Biomed Eng 30, 305–314.